LETTER

doi:10.1038/nature11782

Exaggerated translation causes synaptic and behavioural aberrations associated with autism

Emanuela Santini[1], Thu N. Huynh[1], Andrew F. MacAskill[1], Adam G. Carter[1], Philippe Pierre[2,3,4], Davide Ruggero[5]*, Hanoch Kaphzan[1]†* & Eric Klann[1]

Autism spectrum disorders (ASDs) are an early onset, heterogeneous group of heritable neuropsychiatric disorders with symptoms that include deficits in social interaction skills, impaired communication abilities, and ritualistic-like repetitive behaviours[1,2]. One of the hypotheses for a common molecular mechanism underlying ASDs is altered translational control resulting in exaggerated protein synthesis[3]. Genetic variants in chromosome 4q, which contains the *EIF4E* locus, have been described in patients with autism[4,5]. Importantly, a rare single nucleotide polymorphism has been identified in autism that is associated with increased promoter activity in the *EIF4E* gene[6]. Here we show that genetically increasing the levels of eukaryotic translation initiation factor 4E (eIF4E) in mice[7] results in exaggerated cap-dependent translation and aberrant behaviours reminiscent of autism, including repetitive and perseverative behaviours and social interaction deficits. Moreover, these autistic-like behaviours are accompanied by synaptic pathophysiology in the medial prefrontal cortex, striatum and hippocampus. The autistic-like behaviours displayed by the eIF4E-transgenic mice are corrected by intracerebroventricular infusions of the cap-dependent translation inhibitor 4EGI-1. Our findings demonstrate a causal relationship between exaggerated cap-dependent translation, synaptic dysfunction and aberrant behaviours associated with autism.

eIF4E-transgenic mice (βT-*Eif4e*)[7] exhibited increased levels of eIF4E across brain regions (Fig. 1a) without compensatory changes in levels of other translational control proteins (Fig. 1b). We investigated whether eIF4E was bound preferentially to either eIF4E-binding protein (4E-BP) or eIF4G, which repress and promote, respectively, the initiation of cap-dependent translation[8,9]. We found significantly higher levels of eIF4E–eIF4G interactions in the brains of eIF4E-transgenic mice (Fig. 1c and Supplementary Fig. 1a), with no alterations in the interaction between eIF4E and 4E-BP (Fig. 1c, left, and Supplementary Fig. 1a). To confirm that the increased eIF4E–eIF4G interactions resulted in increased protein synthesis, we infused puromycin into the lateral ventricle of cannulated mice and labelled newly synthesized proteins using SUnSET[10,11], and observed increased *de novo* cap-dependent translation (Fig. 1d and Supplementary Fig. 1b–g). Overall, our results indicate that overexpression of eIF4E results in exaggerated cap-dependent translation in the brains of eIF4E-transgenic mice.

We then determined whether eIF4E-transgenic mice display repetitive and perseverative behaviours, which are behavioural domains required for ASD diagnosis[2]. eIF4E-transgenic mice exhibited repetitive digging behaviour in the marble-burying test[12] and increased self-grooming[13] compared with wild-type littermate controls (Fig. 2a, b). eIF4E-transgenic mice also displayed cognitive inflexibility in both a water-based Y-maze task and a modified version of the Morris water maze[14,15]. Learning ability in the acquisition and memory phases of these tasks was intact; however, in the reversal phases, eIF4E-transgenic mice were impaired in locating the new platform positions (Fig. 2c, d and Supplementary Fig. 2e–h). We tested an additional form of behavioural inflexibility by examining the eIF4E-transgenic mice for extinction of cued fear conditioning and found that they did not exhibit a significant reduction in freezing responses after extinction training (Fig. 2e). These experiments suggest that excessive cap-dependent translation in the brain affects the ability to suppress previously codified response patterns and the ability to form new behavioural strategies in response to changed environmental circumstances.

Abnormalities in social interaction skills are another behavioural defect displayed by individuals with ASDs[2]. In tests to examine social behaviour[16–18], the eIF4E-transgenic mice did not show a preference for a nonspecific stranger versus a new, inanimate object (Fig. 2f, g). Moreover, eIF4E-transgenic mice exhibited diminished reciprocal interactions with a freely moving stranger mouse (Fig. 2h), further evidence of deficits in social behaviour. The deficits in social behaviour of the eIF4E-transgenic mice are unlikely to be caused by a generalized increase in anxiety (Supplementary Fig. 2c, d, j). Moreover, the eIF4E-transgenic mice exhibited mild hyperactivity (Supplementary Fig. 2a, b), but no impairments in motor coordination, motor learning and sensorimotor gating (Supplementary Fig. 2i, k, l). Taken together, our behavioural analysis of the eIF4E-transgenic mice indicates that increased cap-dependent translation in the brain results in a distinct pattern of behavioural abnormalities consistent with ASDs.

Previous studies suggest that ASD symptoms such as cognitive inflexibility and deficits in social behaviour are generated by abnormalities in prefrontal and/or striatal circuits[19]. Consistent with this idea, the medial prefrontal cortex (PFC) is implicated in the modulation of social behaviours and social skills[20], whereas motor, social and communication impairments in boys with ASDs are associated with anatomical abnormalities in the striatum[21]. Therefore, we next examined whether the eIF4E-transgenic mice exhibited specific synaptic pathophysiologies in the medial PFC and striatum.

In the eIF4E-transgenic mice, examination of spontaneous synaptic 'mini' events in layers 2/3 of acute medial PFC slices revealed an increase in the frequency but not amplitude of excitatory events (miniature excitatory postsynaptic currents (mEPSCs); Fig. 3a), and an increase in the amplitude, but not frequency, of inhibitory events (miniature inhibitory postsynaptic currents (mIPSCs); Fig. 3b). No changes were observed in layer 5 (Supplementary Fig. 3a, b). Thus, our data suggest an enhancement of excitatory input and postsynaptic sensitivity for inhibitory events onto layer 2/3 pyramidal neurons, consistent with the hypothesis that autism may arise from an imbalance between excitatory and inhibitory synaptic transmission[22].

To determine whether the increased frequency of spontaneous mEPSCs might result from an enhanced number of synaptic contacts, we imaged dendritic spines using two-photon laser-scanning

[1]Center for Neural Science, New York University, New York, New York 10003, USA. [2]Centre d'Immunologie de Marseille-Luminy, Aix-Marseille Université, Marseille 13288, France. [3]INSERM, U1104, Marseille 13288, France. [4]CNRS, URM 7280, Marseille 13288, France. [5]Department of Urology, School of Medicine, Helen Diller Family Comprehensive Cancer Center, University of California, San Francisco, San Francisco, California 94143, USA. †Present address: Sagol Department of Neurobiology, Faculty of Natural Sciences, University of Haifa, Haifa 31095, Israel.
*These authors contributed equally to this work.

©2013 Macmillan Publishers Limited. All rights reserved

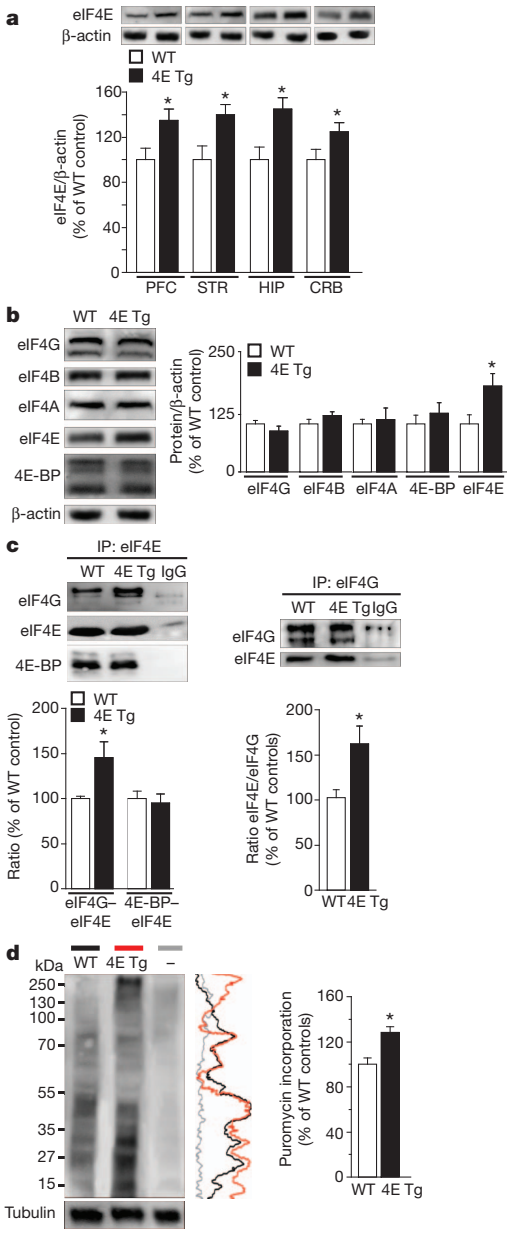

Figure 1 | eIF4E-transgenic mice exhibit increased eIF4E/eIF4G interactions and exaggerated cap-dependent translation. **a**, eIF4E-transgenic mice (4E Tg) exhibit increased eIF4E expression in multiple brain regions. $n = 4$ mice per genotype; $^*P < 0.05$ versus wild type (WT), Student's *t*-test. CRB, cerebellum; HIP, hippocampus; PFC, prefrontal cortex; STR, striatum. **b**, eIF4E-transgenic mice exhibit normal expression of other translational control proteins. $n = 4$ mice per genotype; $^*P < 0.05$, Student's *t*-test. **c**, eIF4E-transgenic mice exhibit increased eIF4E–eIF4G interactions. Immunoprecipitation (IP) of eIF4E (left) and eIF4G (right). $n = 3$ mice per genotype; $^*P < 0.05$, Student's *t*-test. **d**, eIF4E-transgenic mice exhibit increased translation as measured with SUnSET (see Methods). Vertical line traces of each autoradiogram are shown on the right. $n = 3$ mice per genotype; $^*P < 0.05$, Student's *t*-test. '–' represents a control sample without puromycin. All data are shown as mean and s.e.m.

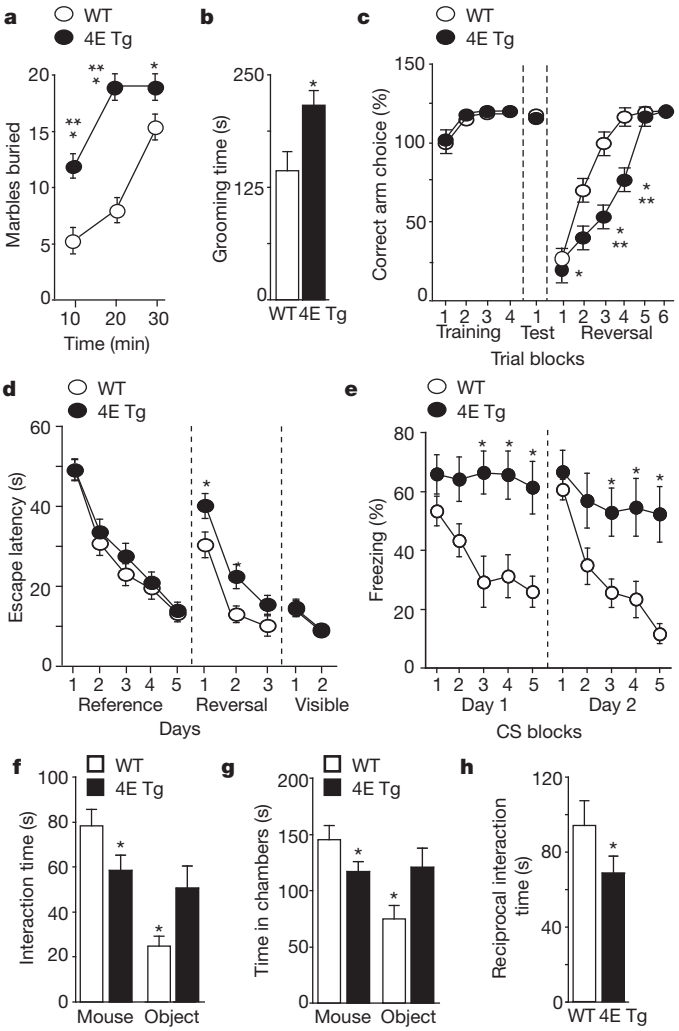

Figure 2 | eIF4E-transgenic mice exhibit ASD-like behaviours. eIF4E-transgenic mice were compared to wild-type littermates. **a**, Marble-burying test. $n = 21$–22 mice per genotype; $^*P < 0.05$, $^{***}P < 0.001$, repeated-measures analysis of variance (ANOVA) (time × genotype, $F_{(2,46)} = 31.62$, $P < 0.001$) followed by Bonferroni–Dunn post-hoc test. **b**, Self-grooming test. $n = 12$ mice per genotype; $^*P < 0.05$, Student's *t*-test. **c**, Y-maze reversal task. $n = 21$–22 mice per genotype; $^*P < 0.05$, $^{***}P < 0.001$, repeated-measures ANOVA (time × genotype, $F_{(5,138)} = 16.74$, $P < 0.001$) followed by Bonferroni–Dunn post-hoc test. **d**, Morris water maze reversal learning. $n = 12$–13 mice per genotype; $^*P < 0.05$, repeated-measures ANOVA (time × genotype, $F_{(3,92)} = 6.1$, $P < 0.001$) followed by Bonferroni–Dunn post-hoc test. **e**, Extinction of cued fear memory (15 conditioned stimuli (CS) per day represented as three CS blocks). $n = 6$ mice per genotype; $^*P < 0.05$, repeated-measures ANOVA (day 1: time × genotype, $F_{(4,40)} = 5.73$, $P < 0.001$; day 2: time × genotype, $F_{(4,40)} = 4.81$, $P < 0.01$) followed by Bonferroni–Dunn post-hoc test. **f**, **g**, Social behaviour test. The time spent either interacting with a stranger mouse (**f**) or in the chambers (**g**). $n = 6$ mice per genotype; $^*P < 0.05$, repeated-measures ANOVA (stimulus × genotype, $F_{(1,10)} = 6.04$, $P < 0.05$ (**f**); stimulus × genotype, $F_{(1,10)} = 6.12$, $P < 0.05$ (**g**)) followed by Bonferroni–Dunn post-hoc test. **h**, Reciprocal social interaction task. $n = 6$ mice per genotype; $^*P < 0.05$, Student's *t*-test. All data are shown as mean and s.e.m.

microscopy (Fig. 3c, d and Supplementary Fig. 3c, d). We found a significant increase (~12%) in spine density and observed a significantly smaller spine volume in the eIF4E-transgenic mice than in wild-type littermates (wild type = $0.123 \pm 0.004\ \mu m^3$ (mean ± s.e.m.) and eIF4E-transgenic = $0.110 \pm 0.004\ \mu m^3$, $P = 0.01$ versus wild type, Student's *t*-test).

Next, we examined whether increased expression of eIF4E also resulted in synaptic pathophysiology in the striatum. We used high-frequency stimulation to induce long-term depression (LTD) in acute striatal slices[23], and found that eIF4E-transgenic mice exhibited enhanced LTD compared to wild-type littermates (Fig. 3e and Supplementary Fig. 3e, f). We propose that the enhanced LTD in eIF4E-transgenic mice results in altered efficiency of striatal information storage and processing, culminating in the inability to form new motor patterns and/or to disengage from previously learned motor behaviours.

©2013 Macmillan Publishers Limited. All rights reserved

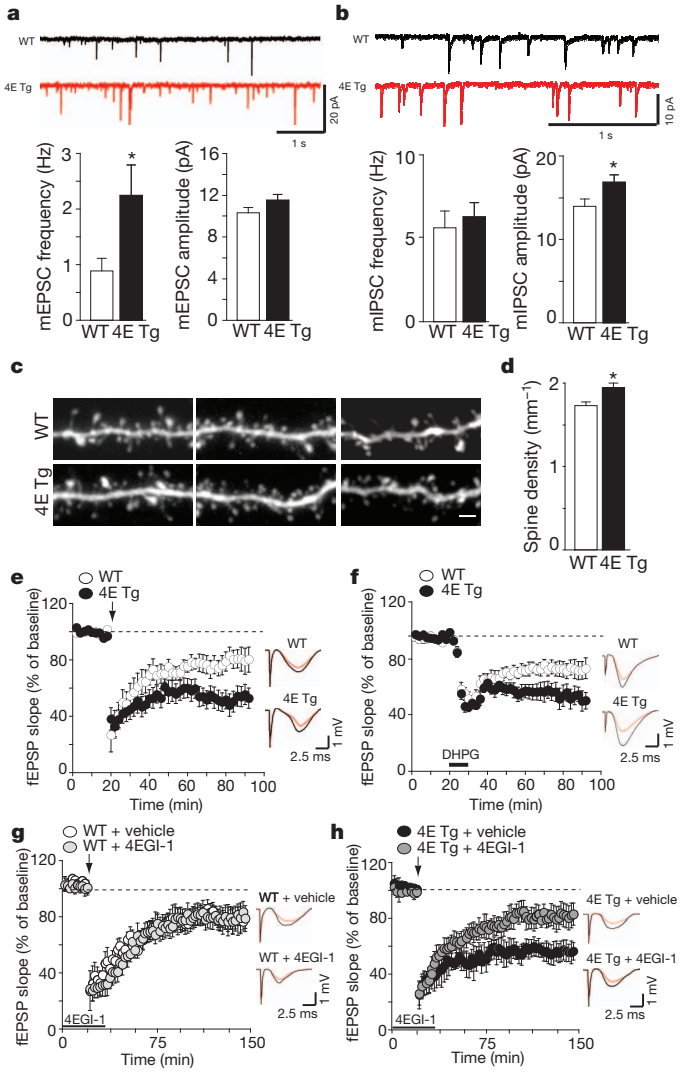

Figure 3 | eIF4E-transgenic mice exhibit alterations in synaptic function, dendritic spine density and synaptic plasticity. **a**, **b**, eIF4E-transgenic mice exhibit increased mEPSC frequency (**a**) and increased mIPSC amplitude (**b**) in layer 2/3 medial PFC pyramidal neurons. $n = 27–30$ neurons per genotype; $^*P < 0.05$, Student's t-test. **c**, **d**, eIF4E-transgenic mice exhibit increased dendritic spine density in layer 2/3 medial PFC pyramidal neurons. High-magnification images (**c**) and quantification (**d**) of spiny dendrites. $n = 12$ neurons per genotype; $^*P < 0.05$, Student's t-test. Scale bar, 2 μm. **e**, eIF4E-transgenic mice exhibit enhanced striatal LTD. $n = 13$ slices from 8 mice per genotype. **f**, eIF4E-transgenic mice exhibit enhanced hippocampal mGluR-LTD. DHPG denotes the mGluR agonist 3,5-dihydroxyphenylglycine. $n = 15$ slices from 8 mice per genotype. **g**, **h**, 4EGI-1 normalizes enhanced striatal LTD shown by eIF4E-transgenic mice (**h**), without affecting LTD in wild-type mice (**g**). $n = 18$ slices from 9 mice per genotype and treatment. All field recordings were analysed with repeated-measures ANOVA. Arrows indicate delivery of high-frequency stimulation. Solid bars indicate the duration of bath application of DHPG (10 μM, 10 min) and 4EGI-1 (100 μM, 45 min). Representative traces (right) showing field excitatory postsynaptic potentials (fEPSPs) before (black) and 60 min after (red) high-frequency stimulation. All data are shown as mean and s.e.m.

To determine whether the synaptic alterations described in the eIF4E-transgenic mice were selective for the frontostriatal circuit, we examined synaptic plasticity in the hippocampus[24]. We found that eIF4E-transgenic mice exhibited enhanced metabotropic glutamate receptor-dependent LTD (mGluR-LTD) compared to wild-type littermates (Fig. 3f and Supplementary Fig. 3g, h), consistent with previous studies showing that changes in brain protein synthesis are accompanied by altered (enhanced or reduced) hippocampal mGluR-LTD[25,26]. Thus, consistent with the ubiquitous increase in brain expression of eIF4E, the eIF4E-transgenic mice display altered synaptic function and plasticity in several brain regions (medial PFC, striatum and hippocampus) implicated in behavioural abnormalities associated with ASDs.

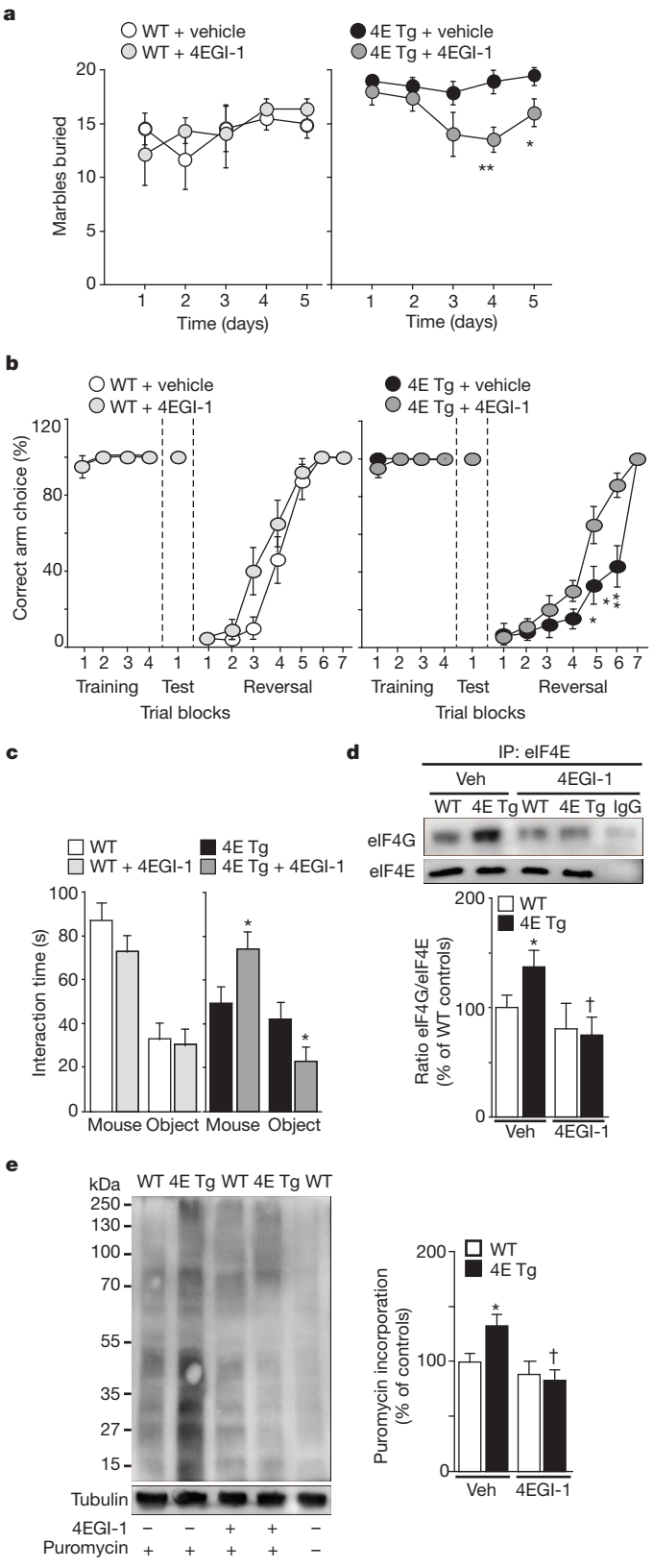

©2013 Macmillan Publishers Limited. All rights reserved

Figure 4 | The cap-dependent translation inhibitor 4EGI-1 reverses ASD-like behaviours shown by eIF4E-transgenic mice. **a**, Treatment of eIF4E-transgenic mice with 4EGI-1 reduces the marble-burying behaviour. $n = 6$ mice per genotype and treatment; $^{*}P < 0.05$, $^{**}P < 0.01$, two-way repeated-measures ANOVA (treatment × genotype, $F_{(1,20)} = 4.21$, $P < 0.05$) followed by Bonferroni–Dunn post-hoc test. **b**, 4EGI-1 improves the cognitive flexibility of eIF4E-transgenic mice in the Y-maze test. $n = 6$–7 mice per genotype and treatment; $^{*}P < 0.05$, $^{**}P < 0.01$, two-way repeated-measures ANOVA (treatment × genotype, $F_{(1,21)} = 4.61$, $P < 0.05$) followed by Bonferroni–Dunn post-hoc test. **c**, 4EGI-1 improves social behaviour of eIF4E-transgenic mice in the three-chamber arena test. $n = 6$ mice per genotype and treatment; $^{*}P < 0.05$, two-way repeated-measures ANOVA (treatment × genotype, $F_{(1,20)} = 6.26$, $P < 0.05$) followed by Bonferroni–Dunn post-hoc test. **d**, 4EGI-1 decreases the enhanced eIF4E–eIF4G interactions in eIF4E-transgenic mice. Immunoprecipitation of eIF4E in the striatum. $n = 4$ mice per genotype; $^{*}P < 0.05$ (versus vehicle-treated wild type), $^{\dagger}P < 0.05$ (versus 4EGI-1-treated wild type), two-way ANOVA, followed by Bonferroni–Dunn post-hoc test. **e**, 4EGI-1 normalizes the exaggerated cap-dependent translation in eIF4E-transgenic mice as measured with SUnSET. The last wild-type sample represents a control without puromycin. $^{*}P < 0.05$, $^{\dagger}P < 0.05$, two-way ANOVA followed by Bonferroni–Dunn post-hoc test. All data are shown as mean and s.e.m.

Finally, we asked whether exaggerated cap-dependent translation was responsible for the synaptic alterations and ASD-like behaviours shown by the eIF4E-transgenic mice. We took advantage of 4EGI-1, an inhibitor of eIF4E–eIF4G interactions[8,11], to block the synaptic and behavioural consequences of increased eIF4E expression. Bath application of 4EGI-1 normalized the enhanced striatal LTD observed in the eIF4E-transgenic mice (Fig. 3g, h), suggesting that exaggerated striatal LTD (Fig. 3h) is a direct consequence of increased binding of eIF4E to eIF4G (Supplementary Fig. 3i–k).

Next, we used a subthreshold dose of 4EGI-1 (ref. 11) to normalize the behavioural abnormalities in eIF4E-transgenic mice without impairing their wild-type littermates. eIF4E-transgenic mice treated with 4EGI-1 exhibited a decrease in repetitive behaviour during the marble-burying task, which started on day four and persisted throughout day five (Fig. 4a). Moreover, we found that 4EGI-1 maintained the behavioural effects observed in the marble-burying task (Supplementary Fig. 4a, b). We also found that blockade of eIF4E–eIF4G interactions with 4EGI-1 significantly improved the performance of eIF4E-transgenic mice in the reversal phase of the Y-maze test (Fig. 4b). These findings indicate that chronic treatment of eIF4E-transgenic mice with 4EGI-1 reverses their repetitive and perseverative behaviours. We also found that infusions of 4EGI-1 rescued the social behaviour deficits shown by the eIF4E-transgenic mice in the three-chamber arena test, as they exhibited an increased preference for a nonspecific stranger compared to a new object (Fig. 4c).

At the completion of the behavioural studies with 4EGI-1, we performed co-immunoprecipitation experiments, confirming that 4EGI-1 reduced the increased eIF4E–eIF4G interactions exhibited by the eIF4E-transgenic mice (Fig. 4d and Supplementary Fig. 4c–e). Furthermore, puromycin-labelling of newly synthesized proteins was reduced to wild-type levels, indicating that 4EGI-1 was effective in attenuating the increased cap-dependent translation in the eIF4E-transgenic mice (Fig. 4e and Supplementary Fig. 4f, g). Together, these results indicate that repeated treatment of eIF4E-transgenic mice with 4EGI-1 reverses the increased binding of eIF4E to eIF4G, exaggerated cap-dependent translation, and reversal of ASD-like behaviours.

Here we have demonstrated that increased eIF4E expression and, consequently, dysregulated translational control at the initiation phase of protein synthesis in mice results in the appearance of synaptic dysfunction and aberrant behaviours consistent with ASDs. On the basis of our observations, we propose that exaggerated cap-dependent protein synthesis in the eIF4E-transgenic mice and fragile X syndrome model mice[27,28] results in enhanced translation of a specific subset of messenger RNAs. Thus, the identity of both these mRNAs and the *cis*-acting elements in the 5′ untranslated region responsible for eIF4E-dependent protein synthesis and their possible overlap with fragile X mental retardation protein target mRNAs will be important investigations in future studies.

Our studies with eIF4E-transgenic mice indicate that ASD-like behaviours can be induced by exaggerated cap-dependent translation in the brain. Moreover, we demonstrated that aberrant repetitive, perseverative and social behaviours shown by eIF4E-transgenic mice are reversed by reducing eIF4E–eIF4G interactions, thereby restoring translational homeostasis. Thus, our findings establish a causal link between exaggerated cap-dependent translation and behaviours associated with autism. Finally, our findings indicate that behavioural defects caused by exaggerated cap-dependent translation, which also occurs in fragile X syndrome[29,30], a disorder with a high incidence of autism, are not irrevocable and can be corrected well into adulthood.

METHODS SUMMARY

All procedures involving animals were approved by the New York University Animal Care and Use Committee and followed the National Institutes of Health Guidelines for the use of animals in research. For a detailed description of all the techniques used in this study, please see the Methods. All the experiments were performed with the examiners blinded to genotype.

Full Methods and any associated references are available in the online version of the paper.

Received 23 January; accepted 12 November 2012.
Published online 23 December 2012.

1. Levitt, P. & Campbell, D. B. The genetic and neurobiologic compass points toward common signaling dysfunctions in autism spectrum disorders. *J. Clin. Invest.* **119,** 747–754 (2009).
2. Rapin, I. & Tuchman, R. F. Autism: definition, neurobiology, screening, diagnosis. *Pediatr. Clin. North Am.* **55,** 1129–1146 (2008).
3. Kelleher, R. J. & Bear, M. F. The autistic neuron: troubled translation? *Cell* **135,** 401–406 (2008).
4. The Autism Genome Project Consortium. Mapping autism risk loci using genetic linkage and chromosomal rearrangements. *Nature Genet.* **39,** 319–328 (2007).
5. Yonan, A. L. *et al.* A genomewide screen of 345 families for autism-susceptibility loci. *Am. J. Hum. Genet.* **73,** 886–897 (2003).
6. Neves-Pereira, M. *et al.* Deregulation of *EIF4E*: a novel mechanism for autism. *J. Med. Genet.* **46,** 759–765 (2009).
7. Ruggero, D. *et al.* The translation factor eIF-4E promotes tumor formation and cooperates with c-Myc in lymphomagenesis. *Nature Med.* **10,** 484–486 (2004).
8. Moerke, N. J. *et al.* Small-molecule inhibition of the interaction between the translation initiation factors eIF4E and eIF4G. *Cell* **128,** 257–267 (2007).
9. Gingras, A. C. *et al.* Hierarchical phosphorylation of the translation inhibitor 4E–BP1. *Genes Dev.* **15,** 2852–2864 (2001).
10. Schmidt, E. K., Clavarino, G., Ceppi, M. & Pierre, P. SUnSET, a nonradioactive method to monitor protein synthesis. *Nature Methods* **6,** 275–277 (2009).
11. Hoeffer, C. A. *et al.* Inhibition of the interactions between eukaryotic initiation factors 4E and 4G impairs long-term associative memory consolidation but not reconsolidation. *Proc. Natl Acad. Sci. USA* **108,** 3383–3388 (2011).
12. Thomas, A. *et al.* Marble burying reflects a repetitive and perseverative behavior more than novelty-induced anxiety. *Psychopharmacology (Berl.)* **204,** 361–373 (2009).
13. Peça, J. *et al.* Shank3 mutant mice display autistic-like behaviours and striatal dysfunction. *Nature* **472,** 437–442 (2011).
14. Hoeffer, C. A. *et al.* Removal of FKBP12 enhances mTOR-Raptor interactions, LTP, memory, and perseverative/repetitive behavior. *Neuron* **60,** 832–845 (2008).
15. Ehninger, D. *et al.* Reversal of learning deficits in a *Tsc2*$^{+/-}$ mouse model of tuberous sclerosis. *Nature Med.* **14,** 843–848 (2008).
16. Moy, S. S. *et al.* Sociability and preference for social novelty in five inbred strains: an approach to assess autistic-like behavior in mice. *Genes Brain Behav.* **3,** 287–302 (2004).
17. Zhou, J. *et al.* Pharmacological inhibition of mTORC1 suppresses anatomical, cellular, and behavioral abnormalities in neural-specific Pten knock-out mice. *J. Neurosci.* **29,** 1773–1783 (2009).
18. Kwon, C.-H. *et al.* Pten regulates neuronal arborization and social interaction in mice. *Neuron* **50,** 377–388 (2006).
19. Fineberg, N. A. *et al.* Probing compulsive and impulsive behaviors, from animal models to endophenotypes: a narrative review. *Neuropsychopharmacology* **35,** 591–604 (2010).
20. Yizhar, O. *et al.* Neocortical excitation/inhibition balance in information processing and social dysfunction. *Nature* **477,** 171–178 (2011).
21. Qiu, A., Adler, M., Crocetti, D., Miller, M. I. & Mostofsky, S. H. Basal ganglia shapes predict social, communication, and motor dysfunctions in boys with autism spectrum disorder. *J. Am. Acad. Child Adolesc. Psychiatry* **49,** 539–551 (2010).
22. Tabuchi, K. *et al.* A neuroligin-3 mutation implicated in autism increases inhibitory synaptic transmission in mice. *Science* **318,** 71–76 (2007).
23. Calabresi, P., Maj, R., Pisani, A., Mercuri, N. B. & Bernardi, G. Long-term synaptic depression in the striatum: physiological and pharmacological characterization. *J. Neurosci.* **12,** 4224–4233 (1992).

©2013 Macmillan Publishers Limited. All rights reserved

24. Hou, L. *et al.* Dynamic translational and proteasomal regulation of fragile X mental retardation protein controls mGluR-dependent long-term depression. *Neuron* **51,** 441–454 (2006).
25. Huber, K. M., Kayser, M. S. & Bear, M. F. Role for rapid dendritic protein synthesis in hippocampal mGluR-dependent long-term depression. *Science* **288,** 1254–1256 (2000).
26. Auerbach, B. D., Osterweil, E. K. & Bear, M. F. Mutations causing syndromic autism define an axis of synaptic pathophysiology. *Nature* **480,** 63–68 (2011).
27. Ronesi, J. A. *et al.* Disrupted Homer scaffolds mediate abnormal mGluR5 function in a mouse model of fragile X syndrome. *Nature Neurosci.* **15,** 431–440 (2012).
28. Sharma, A. *et al.* Dysregulation of mTOR signaling in fragile X syndrome. *J. Neurosci.* **30,** 694–702 (2010).
29. Dölen, G. *et al.* Correction of fragile X syndrome in mice. *Neuron* **56,** 955–962 (2007).
30. Qin, M., Kang, J., Burlin, T. V., Jiang, C. & Smith, C. B. Postadolescent changes in regional cerebral protein synthesis: an *in vivo* study in the *Fmr1* null mouse. **25,** 5087–5095 (2005).

Supplementary Information is available in the online version of the paper.

Acknowledgements We would like to thank J. LeDoux and members of his laboratory for their technical support and suggestions. We would also like to thank D. St Clair and Z. Miedzybrodzka for their comments on the manuscript. This research was supported by National Institutes of Health (NIH) grants NS034007, NS047384 and NS078718, and Department of Defense CDMRP award W81XWH-11-1-0389 (E.K.), NIH grant CA154916 (D.R.) and the Wellcome Trust (A.F.M.).

Author Contributions The study was directed by E.K. and conceived and designed by E.S. and E.K. E.S. performed the molecular, behavioural and electrophysiological experiments. T.N.H. performed behavioural experiments. A.F.M. and A.G.C. performed the dendritic spine-density experiments. P.P. contributed the anti-puromycin (12D10) antibody. D.R. contributed with reagents and expertise concerning translation control by eIF4E. H.K. performed the cortical whole-cell electrophysiological experiments. The manuscript was written by E.S. and E.K. and edited by all of the authors.

Author Information Reprints and permissions information is available at www.nature.com/reprints. The authors declare no competing financial interests. Readers are welcome to comment on the online version of the paper. Correspondence and requests for materials should be addressed to E.K. (eklann@cns.nyu.edu).

©2013 Macmillan Publishers Limited. All rights reserved

METHODS

Housing. Generation of βT-*Eif4e* transgenic mice (eIF4E-transgenic mice) has been described previously[7].

For all the experiments, we made use of littermates derived from crossing heterozygotes. Mice were backcrossed to the N10 generation in C57BL/6J mice. Overall, eIF4E-transgenic mice were viable, fertile and showed no gross anatomical abnormalities in the age range used for this study. eIF4E-transgenic mice and their wild-type littermates were housed in groups of 3–4 animals per cage and kept on a regular 12 h light/dark cycle (7:00–19:00 light period). Food and water were available ad libitum.

Surgery and drug infusion. Mice were anaesthetized (ketamine (100 mg kg^{-1}) and xylazine (10 mg kg^{-1})) and mounted onto a stereotaxic apparatus. Cannulae (26-gauge) were implanted unilaterally at the following coordinates: −0.22 mm anterioposterior, +1 mm mediolateral, and −2.4 mm dorsoventral[31]. Mice were allowed 1 week to recover after the surgery.

The infusions of the eIF4E–eIF4G inhibitor 4EGI-1 were performed as described previously[11]. In brief, 4EGI-1 dissolved in 100% dimethylsulphoxide (DMSO) was diluted in vehicle (0.5% (2-hydroxypropyl)-β-cyclodextrin and 1% DMSO in artificial cerebrospinal fluid (ACSF)). Vehicle or 4EGI-1 (20 μM) was infused over 1 min (0.5 μl min^{-1}; Harvard Apparatus). On the last day of treatment, mice received infusion of 4EGI-1 alone or puromycin (25 μg in 0.5 μl) before 4EGI-1 infusions. All behaviour and tissue dissection occurred 1 h after 4EGI-1 infusions.

Behaviour. The following behavioural tests were performed on male eIF4E-transgenic mice and their wild-type littermates (2–6 months of age) as described previously: novelty induced locomotor activity[32], open field[33], elevated plus maze[33], rotarod[34], prepulse inhibition[33], marble[14], social behaviour[16], direct social interaction[35,36], Y-maze and the Morris water maze[7,35].

For all experiments, mice were acclimated to the testing room 30 min before behavioural training and all behaviour apparatuses were cleaned between each trial with 30% ethanol. The experimenter was blinded to genotype and drug treatment while performing and scoring all behavioural tasks. All behavioural tests were performed starting with the least aversive task first (locomotor activity) and ending with the most aversive (either water-based mazes or extinction of fear memory).

Western blots. Mice were killed by decapitation 1 h after the infusion with either 4EGI-1 alone or 4EGI-1 plus puromycin. The striatum and prefrontal cortex were rapidly dissected, placed on an ice-cold surface, and sonicated in 1% SDS and boiled for 10 min. Aliquots (2 μl) of the homogenate were used for protein determination with a BCA (bicinchoninic acid) assay kit (Pierce, Thermo Scientific). Equal amounts of protein (20 μg) for each sample were loaded onto 10% polyacrylamide gels. Proteins were separated by SDS–PAGE and transferred overnight to polyvinylidene difluoride membranes (Immobilon-Psq, Millipore Corporation). The membranes were immunoblotted with antibodies against eIF4E (1:1,000), eIF4G (1:1,000), eIF4B (1:1,000), eIF4A (1:1,000) and 4E-BP (1:1,000) (Cell Signaling Technology). Antibodies against β-actin and tubulin (1:5,000, Cell Signaling Technology) were used to estimate the total amount of proteins. Detection was based on a horseradish peroxidase (HRP)-conjugated secondary antibody (Promega) and chemiluminescence reagent (ECL or ECL plus; GEHealthcare), and visualized using a Kodak 4000MM imager to obtain pixel density values for the band of interest (Carestream). All images were obtained using maximum sensitivity settings with no binning (0–65 K signal range). No images analysed presented saturating signals for the bands of interest (>65 K greyscale value). The amount of each protein was normalized for the amount of the corresponding β-actin or tubulin detected in the sample.

Immunoprecipitation. Tissue was homogenized in ice-cold lysis immunoprecipitation buffer containing (in mM): 40 HEPES, pH 7.5, 150 NaCl, 10 pyrophosphate, 10 glycerophosphate, 1 EDTA and 0.1% CHAPS, protease inhibitor II, phosphatase inhibitor mixture I, II (Sigma-Aldrich). Cleared homogenate (500 μg) was incubated with either anti-eIF4G (2.5 μg) or anti-eIF4E (2.5 μg) (Bethyl Laboratories) and gently shaken overnight at 4 °C. The antibody–lysate mix was incubated with 75 μl IgG bound to agarose beads (Thermo Scientific). The bead–sample slurry was incubated while rocking at 4 °C overnight. Supernatant was removed and saved, and immunoprecipitates were washed three times in lysis buffer, and once in wash buffer (50 mM HEPES, pH 7.5, 40 mM NaCl, 2 mM EDTA). SDS–PAGE buffer was added to the washed immunoprecipitates, which then were resolved on 4 to 12% gradient gels. Efficiency of the immunoprecipitation was determined by examining the supernatant and wash fractions obtained from the procedure on images obtained from Kodak 4000MM imager (see western blots section). Band density values for coimmunoprecipitated eFI4E, eIF4G and 4E-BP were normalized to immunoprecipitated eIF4G or eIF4E.

SUnSET. A protein synthesis assay was performed as previously described using the SUnSET method[11]. Puromycin-treated samples were identified on blots using the mouse monoclonal antibody 12D10 (1:5,000 from a 5 mg ml^{-2} stock). Because only a small fraction of the brain proteins were labelled, signal from blots was identified using ECL-Advance (GEHealthcare).

Electrophysiology. Hippocampal (400 μm), prefrontal and striatal slices (300 μm) for electrophysiology were prepared as described previously[24].

Solution to maintain slices. Cutting solution (in mM): 110 sucrose, 60 NaCl, 3 KCl, 1.25 NaH_2PO_4, 28 $NaHCO_3$, 0.5 $CaCl_2$, 7 $MgCl_2$, 5 glucose and 0.6 ascorbate. ACSF (in mM): 125 NaCl, 2.5 KCl, 1.25 NaH_2PO_4, 25 $NaHCO_3$, 25 D-glucose, 2 $CaCl_2$ and 1 $MgCl_2$. Slices were incubated at room temperature and then were placed in the recording chamber for additional recovery time of 60 min at 33 °C.

Extracellular recordings. Extracellular fEPSPs were recorded as described previously[23,24]. In all the experiments, baseline synaptic transmission was monitored for at least 20 min before LTD induction. Three trains of high-frequency stimulation (3 s duration, 100 Hz frequency at 20 s intervals) were used to induce LTD in striatal slices[23], and 10 min of incubation with DHPG (50 μM) was used to induce mGluR-dependent LTD in hippocampal slices[24]. The slope of fEPSPs was expressed as a percentage of the baseline average before LTD induction.

Intracellular recordings. Medial prefrontal pyramidal cells were illuminated and visualized using a ×60 water-immersion objective mounted on a fixed-stage microscope (BX61-WI, Olympus), and the image was displayed on a video monitor using a charge-coupled device camera (Hamamatsu). Recordings were amplified by multiclamp 700B and digitized by Digidata 1440 (Molecular Devices). The recording electrode was pulled from a borosilicate glass pipette (3–5 MΩ) using an electrode puller (P-97, Sutter Instruments), filled with an internal solution according to the specific experimental requirement, and patched onto the soma. The series resistance of the patch pipette was compensated ~70% and re-adjusted before each experiment. A measured liquid junction potential was corrected by adjusting the pipette offset. All voltage–clamp recordings were low-pass filtered at 10 kHz and sampled at 50 kHz.

Internal solution for mEPSCs (in mM): 120 caesium-methane-sulphonate, 10 HEPES, 10 EGTA, 4 $MgCl_2$, 0.4 NaGTP, 4 MgATP, 10 phosphocreatine and 5 QX-314 (pH adjusted to 7.3 with CsOH, 290 mOsm). Bicuculline 50 μM and tetrodotoxin 1 μM (Tocris) were added to the external ACSF bath solution.

Internal solution for mIPSCs (in mM): 140 CsCl, 10 EGTA, 10 HEPES, 2 $MgCl_2$, 2.0 Mg-ATP, 4 Na_2-ATP, 0.4 Na_2-GTP and 5 QX-314 (pH adjusted to 7.3 with CsOH, 290 mOsm), thus yielding a chloride reversal potential of around 2 mV for the chloride currents. Tetrodotoxin (1 μM), 6,7-dinitroquinoxaline-2,3-dione (DNQX) (40 μM) and D-2-amino-5-phosphonopentanoate (AP5) (50 μM) were added to the ACSF bath solution.

In these conditions, mEPSCs and mIPSCs were recorded in voltage clamp at −70 mV and measured for 120 s and 60 s, respectively.

Dendritic spine morphology. Dendritic spine density experiments were performed as previously described[37,38]. In brief, two-photon imaging was accomplished with a custom microscope and high-resolution stacks ($x = 0.13$ μm, $y = 0.13$ μm, $z = 0.2$ μm per voxel) of dendritic segments throughout the entire cell were taken for morphological analysis in NeuronStudio. Spine-head volume was calculated using a rayburst algorithm. Images were deconvolved before volume measurements using custom routines written in MATLAB (Mathworks).

31. Franklin, K. B. J. & Paxinos, G. *The Mouse Brain in Stereotaxic Coordinates* 3rd edn (Academic, 2007).
32. Errico, F. *et al.* The GTP-binding protein Rhes modulates dopamine signalling in striatal medium spiny neurons. *Mol. Cell. Neurosci.* **37,** 335–345 (2008).
33. Banko, J. L. *et al.* Behavioral alterations in mice lacking the translation repressor 4E-BP2. *Neurobiol. Learn. Mem.* **87,** 248–256 (2007).
34. Borgkvist, A. *et al.* Altered dopaminergic innervation and amphetamine response in adult *Otx2* conditional mutant mice. *Mol. Cell. Neurosci.* **31,** 293–302 (2006).
35. Chévere-Torres, I., Maki, J. M., Santini, E. & Klann, E. Impaired social interactions and motor learning skills in tuberous sclerosis complex model mice expressing a dominant/negative form of tuberin. *Neurobiol. Dis.* **45,** 156–164 (2012).
36. Blundell, J. *et al.* Neuroligin-1 deletion results in impaired spatial memory and increased repetitive behavior. *J. Neurosci.* **30,** 2115–2129 (2010).
37. Dumitriu, D., Rodriguez, A. & Morrison, J. H. High-throughput, detailed, cell-specific neuroanatomy of dendritic spines using microinjection and confocal microscopy. *Nature Protocols* **6,** 1391–1411 (2011).
38. Chalifoux, J. R. & Carter, A. G. GABAB receptors modulate NMDA receptor calcium signals in dendritic spines. *Neuron* **66,** 101–113 (2010).

©2013 Macmillan Publishers Limited. All rights reserved